Clinical Cancer Research

AACR

Upregulation of Notch2 and Six1 Is Associated with Progression of Early-Stage Lung Adenocarcinoma and a More Aggressive Phenotype at Advanced Stages

Takahiro Mimae, Morihito Okada, Man Hagiyama, et al.

Updated Version	Access the most recent version of this article at: doi:10.1158/1078-0432.CCR-11-1946
Supplementary Material	Access the most recent supplemental material at: http://clincancerres.aacrjournals.org/content/suppl/2011/12/21/1078-0432.CCR-11-1946.DC1.html

Cited Articles	This article cites 40 articles, 19 of which you can access for free at: http://clincancerres.aacrjournals.org/content/18/4/945.full.html#ref-list-1

E-mail alerts	Sign up to receive free email-alerts related to this article or journal.
Reprints and Subscriptions	To order reprints of this article or to subscribe to the journal, contact the AACR Publications Department at pubs@aacr.org.
Permissions	To request permission to re-use all or part of this article, contact the AACR Publications Department at permissions@aacr.org.

Human Cancer Biology

Clinical
Cancer
Research

Upregulation of Notch2 and Six1 Is Associated with Progression of Early-Stage Lung Adenocarcinoma and a More Aggressive Phenotype at Advanced Stages

Takahiro Mimae[1,2], Morihito Okada[1], Man Hagiyama[2,3], Yoshihiro Miyata[1], Yasuhiro Tsutani[1], Takao Inoue[3], Yoshinori Murakami[2], and Akihiko Ito[3]

Abstract

Purpose: Lung adenocarcinoma often manifests as tumors with mainly lepidic growth. The size of invasive foci determines a diagnosis of *in situ*, minimally invasive adenocarcinoma, or invasive types and suggests that some adenocarcinomas undergo malignant progression in that order. This study investigates how transcriptional aberrations in adenocarcinoma cells at the early stage define the clinical phenotypes of adenocarcinoma tumors at the advanced stage.

Experimental Design: We comprehensively searched for differentially expressed genes between pre-invasive and invasive cancer cells in one minimally invasive adenocarcinoma using laser capture micro-dissection and DNA microarrays. We screened expression of candidate genes in 11 minimally invasive adenocarcinomas by reverse transcriptase PCR and examined their involvement in preinvasive-to-invasive progression by transfection studies. We then immunohistochemically investigated the presence of candidate molecules in 64 samples of advanced adenocarcinoma and statistically analyzed the findings, together with clinicopathologic variables.

Results: The transcription factors *Notch2* and *Six1* were upregulated in invasive cancer cells in all 11 minimally invasive adenocarcinomas. Exogenous Notch2 transactivated *Six1* followed by *Smad3*, *Smad4*, and *vimentin*, and enlarged the nuclei of NCI-H441 lung epithelial cells. Immunochemical staining for the transcription factors was double positive in the invasive, but not in the lepidic growth component of a third of advanced Ads, and the disease-free survival rates were lower in such tumors.

Conclusions: Paired upregulation of *Notch2* and *Six1* is a transcriptional aberration that contributes to preinvasive-to-invasive adenocarcinoma progression by inducing epithelial–mesenchymal transition and nuclear atypia. This aberration persisted in a considerable subset of advanced adenocarcinoma and conferred a more malignant phenotype on the subset. *Clin Cancer Res; 18(4); 945–55. ©2011 AACR.*

Introduction

Adenocarcinoma is the most widespread histologic subtype of lung cancer in most countries, accounting for almost half of all lung cancers (1). Lung adenocarcinomas, especially advanced tumors, rarely comprise a single histologic component, and more than 90% of lung adenocarcinomas are of the mixed subtype according to the 2004 WHO classification (2). In an effort to address the complex histologic heterogeneity of adenocarcinomas, a new classification has recently been proposed (3). According to it, a small tumor with the lepidic growth pattern is diagnosed as either adenocarcinoma *in situ* or minimally invasive adenocarcinoma, depending on the presence or absence of microinvasion (≤ 5 mm). If a microinvasion focus of a minimally invasive adenocarcinoma becomes overt (overt invasion; > 5mm), the tumor will be then diagnosed as lepidic-predominant invasive adenocarcinoma. As might be predicted from these diagnostic criteria, to clearly distinguish between adenocarcinoma *in situ* and minimally invasive adenocarcinoma, as well as between minimally invasive adenocarcinoma and lepidic-predominant invasive adenocarcinoma can be difficult. Rather, it seems reasonable to consider that a significant subset of these 3 subtypes is biologically serial and that each subtype represents a different stage of adenocarcinoma progression.

The concept of progression from adenocarcinoma *in situ* to minimally invasive adenocarcinoma is widely accepted (4–9). Noguchi and colleagues noted 2 types of small

Authors' Affiliations: [1]Surgical Oncology, Division of Genome Radiobiology and Medicine, Programs for Biomedical Research, Graduate School of Biomedical Sciences, Hiroshima University, Hiroshima; [2]Division of Molecular Pathology, Institute of Medical Science, University of Tokyo, Tokyo; and [3]Department of Pathology, Faculty of Medicine, Kinki University, Osaka, Japan

AACR American Association for Cancer Research **945**

Translational Relevance

Lung adenocarcinomas with mainly lepidic growth component are diagnosed as *in situ*, minimally invasive adenocarcinoma, or lepidic-predominant invasive adenocarcinoma types, depending on the size of invasive foci. In a minimally invasive adenocarcinoma, differentially expressed genes were comprehensively searched between the preinvasive and invasive components, and 2 transcriptional factors, *Notch2* and *Six1*, were identified as genes upregulated in the invasive component in all 11 minimally invasive adenocarcinomas examined. Transfection experiments suggested that Notch2 and Six1 cooperatively induced epithelial–mesenchymal transition of adenocarcinoma cells. Clinicopathologic analyses revealed that upregulation of both Notch2 and Six1 in invasive foci was detected in one-third of 64 lepidic-predominant invasive adenocarcinomas, and these tumors represented an aggressive phenotype. Paired upregulation of *Notch2* and *Six1* seemed to occur during preinvasive-to-invasive adenocarcinoma progression and define a more malignant subset of advanced adenocarcinoma. Notch2 and Six1 are not only useful biomarkers for malignant potential of adenocarcinoma but also can be therapeutic targets in adenocarcinoma.

(maximum diameter, < 2 cm) adenocarcinomas. These are type A (adenocarcinoma *in situ* according to the 2011 classification) that consists entirely of neoplastic cells that grow in lepidic growth pattern and type C (minimally invasive adenocarcinoma according to the 2011 classification) that consists of peripheral lepidic growth and a central microinvasion focus. The 2 types of tumors differ clinicopathologically. (i) After complete resection, patients with type A have 100% disease-specific survival, whereas the 5-year survival rate for patients with type C is 75% (9). (ii) Type C tumors have higher rates of p53 positivity, proliferation, and nuclear atypia than type A (8, 10, 11). Interpreting these data based on the 2011 classification, the microinvasion focus of minimally invasive adenocarcinoma is considered to develop due to the malignant progression of noninvasive, *in situ* neoplastic cells of the lepidic growth component. In contrast to the development of type C or minimally invasive adenocarcinoma tumors, the progression of minimally invasive adenocarcinoma to more advanced forms, including lepidic-predominant invasive adenocarcinoma, has not been studied in detail.

Genetic studies of adenocarcinoma progression have found mutations in *KRAS* and *EGFR* at the preinvasive stage, such as atypical adenomatous hyperplasia and adenocarcinoma *in situ* (12–15), and some adenocarcinomas have the amplification of these genes at the later stage of invasion and metastasis (7, 16, 17). Besides such genomic alterations, specific transcriptional pathways seem to become upregu-

lated during the progression of adenocarcinoma, because recent findings have increasingly clarified that lung cancer progression is promoted by epithelial–mesenchymal transition (EMT; ref. 18) that is controlled by a group of transcription factors that includes Slug, which is a zinc finger type (19). The homeobox transcription factors Oct4 and downstream Nanog both function upstream of Slug to promote EMT in A549 lung adenocarcinoma cells (20). Although lung adenocarcinoma progression is assumed to be a stepwise process triggered by multiple genetic aberrations, which aberration(s) accounts for each process in the stepwise progression requires precise examination.

In this study, we attempted to obtain the genetic evidence, indicating that all or a subset of lepidic-predominant invasive adenocarcinoma develops from minimally invasive adenocarcinoma, and to clarify what clinical phenotypes the subset has. For this purpose, we designed the experiments that were composed of 3 parts. In the first part, we aimed to comprehensively compare the gene expression profiles between lepidic growth and microinvasion cancer cells from a single minimally invasive adenocarcinoma and successfully identified 2 transcription factors *Notch2* and *Six1* as genes upregulated in microinvasion cells. In the second part, we examined whether the identified genes might play causative roles in early-stage adenocarcinoma progression from lepidic growth to microinvasion cells, and found that Notch2 and Six1 coordinately induced EMT and nuclear atypia in lung epithelial cells. Finally in the third part, we immunohistochemically stained 64 specimens of lepidic-predominant invasive adenocarcinoma for Notch2 and Six1 and found that a third were a simple advanced form of minimally invasive adenocarcinoma, judging from the upregulation of Notch2 and Six1 in overt invasion cells. Importantly, the disease-free survival of patients with such tumors was poorer.

Materials and Methods

Sample selection

This study included patients with both consolidated lung tumors and ground glass opacities on chest high-resolution computed tomography images who underwent lobectomy or segmentectomy at Hiroshima University Hospital between 2007 and 2010 (Hiroshima, Japan). All patients provided written, informed consent to participate in this study and our Institutional Review Board approved the protocol (approval number: Hi-29). Half of the cancerous tissues were placed in Ultramount Aqueous Permanent Mounting Medium (DakoCytomation) and frozen for later studies, whereas the other half was preserved in 10% formalin for diagnosis. Gene expression was analyzed in samples of minimally invasive adenocarcinoma from 11 patients and 64 lepidic-predominant invasive adenocarcinoma tumor samples were immunohistochemically stained.

Cell culture

NCI-H441 human lung papillary adenocarcinoma cells, A549 human lung adenocarcinoma cells and MDA-MB-231

human breast cancer cells were purchased from the American Type Culture Collection and RERF-LC-MS human lung adenocarcinoma cells were from Japanese Cancer Research Resources Bank (JCRB, Osaka, Japan) in 2010, and all experimentation using cell lines proceeded within 6 months after resuscitation. NCI-H441 cells and A549 cells were grown in RPMI-1640 (Nacalai Tesque) and Dulbecco's Modified Eagle Medium (Nacalai Tesque) supplemented with 10% FBS, antibiotics containing 100 units/mL penicillin, 100 µg/mL streptomycin (Invitrogen), and 0.01M-HEPES buffer (Nacalai Tesque) at 37°C in 5% CO_2/95% air. RERF-LC-MS cells were grown in Eagle's minimal essential medium (Nacalai Tesque) supplemented with 10% FBS, antibiotics, and 0.1 mmol/L nonessential amino acids (GIBCO-Invitrogen) at 37°C in 5% CO_2/95% air. MDA-MB-231 cells were grown in L-15 (Sigma-Aldrich) medium supplemented with 10% FBS, antibiotics, and 0.3 g/L L-glutamine (Sigma-Aldrich) at 37°C in 100% air.

Laser capture microdissection

Serial 15-µm sections of the 11 frozen minimally invasive adenocarcinoma tumors were stained with hematoxylin. Only cancer cells were selectively and separately collected from the lepidic growth and microinvasion components using laser capture microdissection (LMD7000; Leica Microsystems GmbH). The cancer cells were placed in the caps of collection tubes containing Tris [2-carboxyethyl] phosphine hydrochloride buffer. The collection time for one slide was 30 minutes. Twenty slides were done for each component. Each cell pool was frozen with dry ice immediately after collection.

RNA purification and amplification with Cy3 or Cy5 labeling

Total RNA was extracted from each cell pool using NucleoSpin RNA XS (Macherey-Nagel GmbH & Co. KG) and from one small (≤ 1 cm) minimally invasive adenocarcinoma tumor and then cDNAs and amino allyl aRNA were synthesized from the RNA using Amino Allyl MessageAmp II aRNA Amplification Kits (Applied Biosystems). CyeDye coupling and fragmentation proceeded according to a protocol supplied by Toray Industries Inc. The concentration, purity, and integrity of the amplified and labeled aRNA were determined using a Eukaryotes Total RNA Nano Series II (Agilent Technologies). Total RNA from cultured cells was also extracted using NucleoSpin RNA XS.

Gene microarray analysis

Amplified RNA samples from microinvasion components were analyzed using 3D-Gene Human Oligo chip 25k (Toray Industries Inc.) microarrays of 25,370 distinct genes and RNA samples from lepidic growth components as controls. The 3-dimensional microarrays were constructed with wells as spaces between probes and cylinder stems with 70-mer oligonucleotide probes on the top to promote efficient hybridization. Cy3- or Cy5-labeled aRNA pools in hybridization buffer were hybridized for 16 hours according to the supplier's protocol (www.3d-gene.com). Hybrid-

ization signals were scanned using ScanArray Express Scanner (PerkinElmer) and processed using GenePixPro version 5.0 (Molecular Devices). Signals detected for each gene were normalized by global normalization (Cy3/Cy5 ratio median = 1) and Cy3/Cy5 normalized ratios >2.0 or <0.5 were, respectively, defined as commonly upregulated or downregulated genes.

Semiquantitative reverse transcriptase PCR

We analyzed the expression of Notch2, Six1, thyroid transcription factor-1 (TTF-1), Smad3, Smad4, vimentin, E-cadherin, and GAPDH mRNA using reverse transcriptase PCR (RT-PCR) using SuperScriptTMIII First-Strand Synthesis SuperMix (Invitrogen) for the RT. In brief, total RNA was incubated with 50 ng of random hexamer primers and 1 µL of annealing buffer at 65°C for 5 minutes. The RNA was then incubated at 25°C for 5 minutes and at 50°C for 50 minutes in a final volume of 20 µL of reaction mixture containing 1× first-strand reaction mix comprising 5 mmol/L $MgCl_2$, 0.5 mmol/L of each deoxynucleotide triphosphate (dNTP), and 2 µL of SuperScriptTMIII/RNaseOUTTM Enzyme Mix.

The cDNA constructs were amplified by PCR using TaKaRa Ex Taq (Takara). The PCR conditions were 35 cycles of 30 seconds at 94°C (denaturation), 30 seconds at 55°C (annealing), and 30 seconds at 72°C (extension). The sense and antisense primers were 5'-AAAAATGGGGCCAACCGA-GAC-3' and 5'-TTCATCCAGAAGGCGCACAA-3' for human Notch2, 5'-ACTCTCTGCTCGGCCCCCTC-3' and 5'-AAGGCTGCTGAAACAGGCGT-3' for human Six1, 5'-ATGTCGATGAGTCCAAAG-3' and 5'-TCACCAGGTCCGA-3' for human TTF-1, 5'-CGGGCCATGGAGCTGTGTGA-3' and 5'-ACCTGCGTCCATGCTGTGGT-3' for human Smad3, 5'-TCAGGGCCTCAGCCAGGACA-3' and 5'-TCTCCTCCA-GAAGGGTCCACGT-3' for human Smad4, 5'-CAAGGGC-CAAGGCAAGTCGC-3' and 5'-GCCGTGAGGTCAGGC-TTGGA-3' for human vimentin, 5'-CCCTGGCTTTGACGCC-GAGA-3' and 5'-AAACGGAGGCCTGATGGGGC-3' for human E-cadherin, and 5'-ACCACAGTCCATGCCATCAC-3' and 5'-TCCACCACCCTGTTGCTGTA-3' for human GAPDH, respectively. The PCR products were resolved by electrophoresis on 1% agarose gels, stained with ethidium bromide, and densitometrically analyzed. The RT-PCR signal intensity was quantified using ImageJ software (NIH) to compare Notch2, Six1, TTF-1, Smad3, Smad4, vimentin, E-cadherin, and GAPDH mRNA levels.

Construction of plasmid vectors expressing Notch2 intracellular domain, TTF-1, and siRNA against Six1

The cDNA construct for Notch2 intracellular domain (ICD; amino acids 1,703–2,475) inserts was amplified by PCR using KOD FX DNA polymerase (Toyobo Co. Ltd.) with following primer set: sense, 5'-CCGGATCCAT-GAAGCGTAAG-3' (containing the first codon of Notch2 ICD); antisense, 5'-CCGTTAACTCACGCATAAACCTG-3' (containing the stop codon of Notch2 ICD). The TTF-1 gene produces 2 alternative transcripts, of which the short form consists of more than 90% of the total transcripts (21). The open reading frame of the short form of the cDNA from

NCI-H441 cells was amplified by PCR using the primer set: sense, 5′-CCGAATTCATGTCGATGAGTCCAAAG-3′; antisense, 5′-CCGTTAACTCACCAGGT-CCGA-3′. The PCR products were resolved by electrophoresis on 1% agarose gels and stained with ethidium bromide. Targeted bands were excised from gels and DNA was extracted and purified using the Wizard SV Gel and PCR Clean-Up System (Promega Corporation), as described by the manufacturer. Extracted DNA chains were annealed and ligated into the BamHI/HpaI (for Notch2) and EcoRI/HpaI (for TTF-1) sites of pCX4-bsr, a modified pCX-bsr retroviral vector (22) provided by Dr. T. Akagi (Osaka Bioscience Institute, Osaka, Japan), and sequenced.

The pSilencer4.1-CMVneo siRNA plasmid vector (Ambion) was used to construct pSilencer4.1-CMVneo-si-Six1 and the negative control, pSilencer4.1-CMVneo-scramble. A DNA chain with the following sense and antisense sequences was synthesized to target the Six1 sequence: 5′-GATCCCCAGCTCAGAAGAGGAATTTTC-AAGAGAAA-TTCCTCTTCTGAGCTGGTT-3′ (sense) and 5′-AGCTTAACCAGCTCAGAAGAGGAATT-TCTCTTGAA-AATTCCTCTTCTGAGCTGGG-3′ (antisense). The target sequence of the negative control (scramble-pSilencer4.1-CMVneo) was 5′-GATCCCGT-CGATTTTGTGATGCTCG-TCAGTTCAAGAGACTGACGAGCATCACAAAATCGACG-G-TT-3′ (sense) and 5′-AGCTTAACGTCGATTTTGTGA-TGCTCGTCAGTCTCTTGAACTGA-CGAGCATCACAAAAT-CGACGG-3′ (antisense), which has no homology with any human DNA. The DNA chains were annealed and ligated into the BamHI/HindIII sites of pSilencer4.1-CMVneo to generate pSilencer4.1-CMVneo-si-Six1. The negative control pSilencer4.1-CMVneo-scramble vector was constructed in the same manner. The plasmids were extracted and the accuracy of the constructs was confirmed by sequencing.

Transfection

NCI-H441 cells were transiently transfected with empty pCX4-bsr, pCX4-bsr-Notch2 ICD, or pCX4-bsr-TTF-1 using FuGENE 6 (Roche Applied Science). In brief, 2.0×10^5 cells were seeded on 60-mm culture dishes overnight until 50% to 80% confluence was reached. Serum-free medium (194 µL) and 6.0 µL of FuGENE 6 reagent were mixed in 1.5-mL tubes and incubated for 5 minutes at room temperature. Plasmid vectors (2.0 µg each) were added and the contents were mixed and incubated with transfection reagent and DNA complex for at least 15 minutes at room temperature. The transfection reagent and DNA complex were added drop wise to the cultured cells and incubated for 48 hours. The medium was removed and the cells were rinsed 3 times with PBS. The transfected cells were then used in various experiments. A549, RERF-LC-MS, and MDA-MB-231 were also transiently transfected with empty pCX4-bsr or pCX4-bsr-Notch2 ICD using FuGENE 6.

Double transfection proceeded as follows. NCI-H441 cells were transiently transfected with 2.0 µg of each of pCX4-bsr-Notch2 ICD and the empty pSilencer4.1-CMVneo, or pSilencer4.1-CMVneo-scramble, or pSilencer4.1-CMVneo -si-Six1 using FuGENE 6.

Immunohistochemistry

Tissues fixed with 10% formalin were embedded in paraffin and cut into 4-µm thick sections that were deparaffinized, rehydrated, and autoclaved for 20 minutes at 121°C in 10 mmol/L citrate buffer (pH 6.0) and then incubated in methanol containing 3% peroxide for 5 minutes. The sections were washed 3 times with PBS between all steps of the procedure. Nonspecific Ig binding in the sections was blocked by incubation with PBS containing 2% bovine serum albumin (BSA) for 10 minutes. The sections were then incubated with anti-Notch2 antibody (ab8926, 1:400 dilution; Abcam) and/or anti-Six1 antibody (HPA001893, 1:100 dilution; Sigma-Aldrich) in PBS containing 2% BSA for 2 hours at room temperature, followed by horseradish peroxidase–conjugated anti-rabbit Ig G antibody (1:100 dilution; Santa Cruz) in PBS containing 2% BSA for 2 hours at 4°C. Color was developed using aminoethylcarbazole (DAB; Dako) as the substrate for peroxidase. Tissues were counterstained with hematoxylin and mounted. Negative immunohistochemical control procedures comprised the omission and replacement of primary antibodies with appropriate concentrations of normal rabbit or mouse IgG. Slides were examined using a light microscope (BX51; Olympus) equipped with a CCD camera DP72 (Olympus). The results on the control slides were negative.

Cancer cells were deemed positive for Notch2 when the cytoplasm of over half of the cancer cells in each of the lepidic growth and microinvasion components was intensely stained. Other staining profiles were defined as negative. Cancer cells were deemed positive for Six1 when nuclei in over half of the cancer cells in each of the lepidic growth and microinvasion components were intensely stained. Other staining profiles were defined as negative.

Nuclear size analysis

Five minimally invasive adenocarcinoma tumors that contained a Notch2-negative lepidic growth component and a Notch2-positive microinvasion component were immunohistochemically selected. The greatest nuclear dimension of cancer cells in both the lepidic growth and microinvasion components was separately determined in 5 tumors using hematoxylin and eosin (H&E) staining and light microscopy (BX51). The greatest nuclear dimension of 200 cells was measured in random fields for each component from each tumor. The greatest nuclear dimension of the control and of NCI-H441 cells transfected in vitro with empty pCX4-bsr, pCX4-bsr-Notch2 ICD, or pCX4-bsr-TTF-1 was assessed by nuclear staining using 4′,6-diamino-2-phenylindole (DAPI) and the fluorescence microscope, Axio Observer D1 (Carl Zeiss). We determined the nuclear dimensions of 100 cells in randomly selected fields in 3 independent experiments.

Statistical analysis

Data about signal intensity and cell morphology are described as means ± SD or as means ± SE and were analyzed using Student t test. The clinicopathologic findings were analyzed using the Mann–Whitney U test for
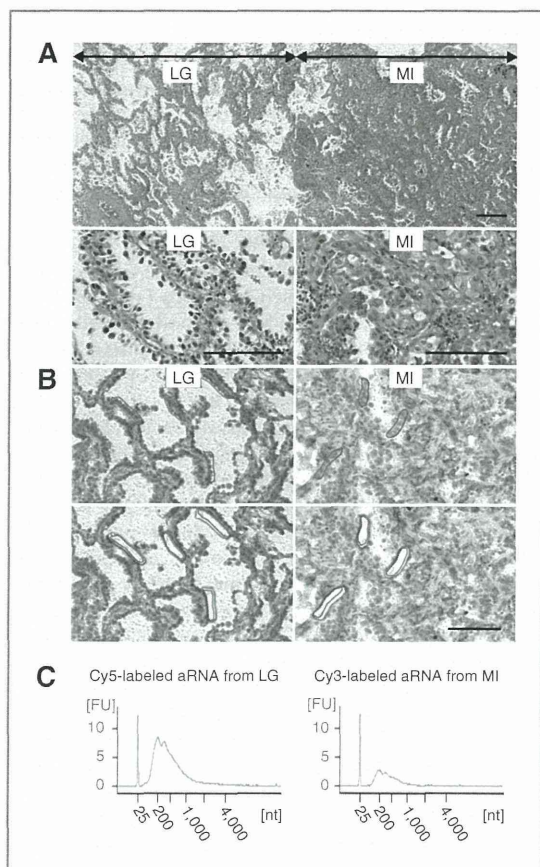
Figure 1. Laser capture microdissection of lepidic growth (LG) and microinvasion (MI) cancer cells from a single minimally invasive adenocarcinoma (case 1) and probe preparation for DNA microarray analysis. A, photomicrograph of minimally invasive adenocarcinoma from case 1 stained with H&E. Top, low-power field view (original magnification, ×100) containing both lepidic growth and microinvasion components; bottom, high-power field view (original magnification, ×400) of each component. B, lepidic growth and microinvasion cancer cells collected by laser capture microdissection from frozen sections of minimally invasive adenocarcinoma tumor. Cancer cells circled in red (top) were cut out using laser pulses run along the circles (bottom). C, verification of aRNA probes for DNA microarray analysis. Total RNA extracted from pools of lepidic growth and microinvasion cancer cells served as templates for preparation of aRNA probes. Quality and quantities of probes were verified by resolving Cy3- or Cy5-labeled aRNA by capillary gel electrophoresis. The amounts of RNA extracted and amplified were 46.2 ng and 14.3 µg for lepidic growth component and 48.4 ng and 4.0 µg for microinvasion component, respectively. Bar, 100 µm.

Results

Isolation of genes that are differentially expressed in lepidic growth and microinvasion cancer cells in a single minimally invasive adenocarcinoma

A small (1 cm in greatest dimension), solitary lung tumor was surgically resected and histopathologically diagnosed as minimally invasive adenocarcinoma (formerly, type C by Noguchi classification; Fig. 1A; case 1 in Fig. 2A and Supplementary Table S1). We separately isolated lepidic growth and microinvasion cancer cells without contamination from frozen tumor sections using a laser capture microdissection system (Fig. 1B). We extracted total RNAs from about 500 lepidic growth and microinvasion cancer cells and then amplified and labeled the RNAs using T7 RNA polymerase. Fig. 1C shows the amounts and quality of the original total RNAs and amplified aRNAs. The aRNAs were comparatively analyzed using highly sensitive oligo DNA microarrays. The complete gene expression dataset of the microdissected minimally invasive adenocarcinoma specimen is available at Gene Expression Omnibus (GEO) accession number GSE30663 (23). The numbers of genes whose expression levels were double or more and half or less in the microinvasion cancer cells were 2,905 and 2,143, respectively. Supplementary Table S2 shows the top 30 of each of
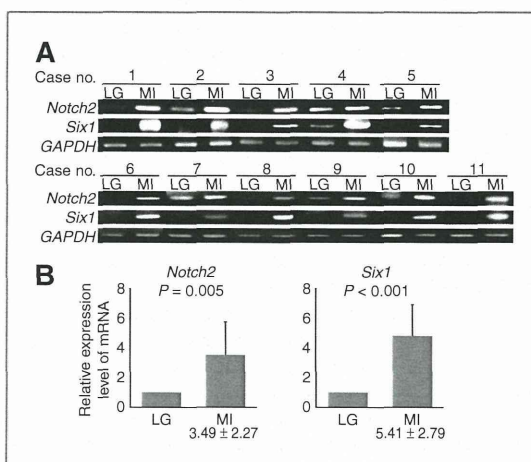

Figure 2. RT-PCR analyses of *Notch2* and *Six1* in total RNA from lepidic growth (LG) and microinvasion (MI) cancer cells in 11 minimally invasive adenocarcinomas. lepidic growth and microinvasion cancer cells were separately collected from frozen sections of minimally invasive adenocarcinomas (cases 1 to 11 listed in Supplementary Table S1) using laser capture microdissection. Total RNAs were extracted from each cell pool and analyzed by RT-PCR using primer sets for *Notch2*, *Six1*, or *GAPDH*. Portions of PCR products were resolved by electrophoresis on 1% agarose gels (A). All band intensities were converted to densitometric values; *Notch2* and *Six1* values were normalized to that of *GAPDH* and then means and SD of 11 minimally invasive adenocarcinomas were calculated. Expression levels of *Notch2* and *Six1* mRNA in microinvasion cancer cells are expressed as relative values normalized to 1 for means in lepidic growth cancer cells (B).

continuous variables and χ^2 tests for categorical variables. Disease-free survival (DFS) curves were calculated using the Kaplan–Meier method. Univariate and multivariate analyses were done using the log-rank and logistic regression tests, respectively. A P value of ≤ 0.05 was regarded as significant.

the upregulated (>94-fold) and downregulated (<1/25.4-fold) candidate genes.

Upregulation of Notch2 and its downstream Six1 in microinvasion cancer cells

We found that *Six1* (136-fold) was the most upregulated among the top 30 genes in microinvasion cancer cells, and *Notch2* was 10.7-fold upregulated in the complete dataset. We considered that this paired upregulation was worthy of further investigation because both Six1 and Notch2 can function as transcription factors and Six1 is a putative downstream target of Notch2 (24, 25). As with minimally invasive adenocarcinoma from case 1, we extracted total RNAs from lepidic growth and microinvasion cancer cells separately from minimally invasive adenocarcinomas resected from cases 2 to 11 (Fig. 2A and Supplementary Table S1). *Six1* and *Notch2* mRNA expression was then screened in all 11 minimally invasive adenocarcinomas by semiquantitative RT-PCR. Significantly more mRNA for either gene was found in microinvasion than in lepidic growth cancer cells from all 11 minimally invasive adeno-carcinomas (Fig. 2A and B). The expression of Notch2 and Six1 proteins was examined in the case 10 minimally invasive adenocarcinoma by immunohistochemistry. Notch2 and Six1 immunoreactive signals were clearly detected in the cytoplasm and nucleus of microinvasion cancer cells, respectively, whereas lepidic growth compo-nent cells were nearly completely negative for the two molecules (Fig. 3).

We speculated whether Notch2 upregulation results in *Six1* transactivation in lung epithelial cells and examined this notion in NCI-H441 cells that have been widely studied as lung epithelial cells. The results of RT-PCR analyses revealed that these cells expressed endogenously undetect-able levels of *Notch2* or *Six1* (Fig. 4A, lane 1). Because Notch2 is enzymatically processed to release its ICD that functions as a transcription factor (26), we subcloned Notch2 ICD cDNA into the mammalian expression vector, pCX4-bsr. NCI-H441 cells transfected with this plasmid contained not only abundant exogenous transcripts for Notch2 ICD but also abundant endogenous transcripts for Six1 (Fig. 4A, lane 3 and Supplementary Fig. S1). We also transfected NCI-H441 cells with the cDNA for TTF-1, well known as a lung epithelial transcription factor, but *Six1* transactivation was undetectable (Fig. 4A, lane 4 and Sup-plementary Fig. S1). Similar experiments using MDA-MB-231 breast cancer cells that express endogenously detectable levels of *Notch2* and *Six1* showed that exogenous Notch2 ICD did not upregulate, but rather slightly downregulated *Six1* (Fig. 4A, lanes 8–10). These results suggested that Notch2 specifically transactivates *Six1* in NCI-H441.

Involvement of Notch2 and Six1 in EMT and nuclear atypism in lung epithelial cells

Notch2 and Six1 promote EMT in various cancers partly through activating the TGF-β intracellular signaling path-ways that involve the intracellular signal transducers Smad3 and Smad4 (27–29). Consistent with their epithelioid
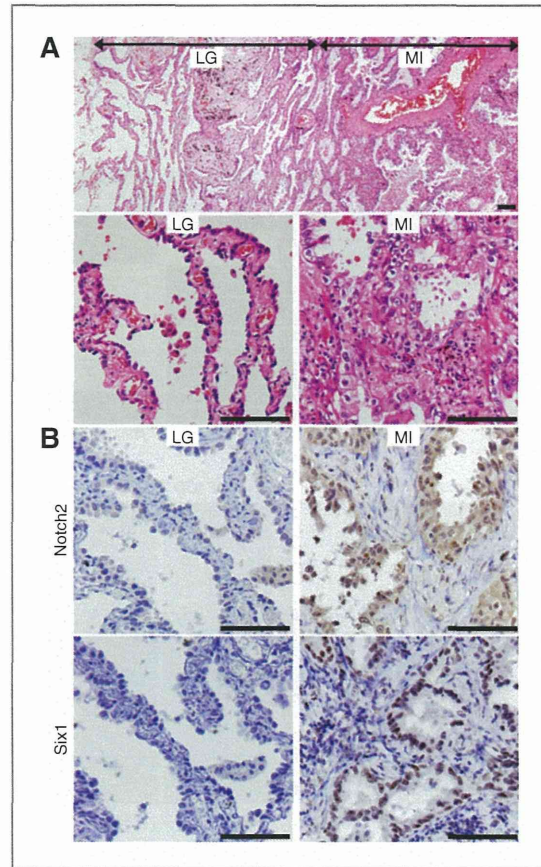

Figure 3. Immunohistochemical staining for Notch2 and Six1 on a minimally invasive adenocarcinoma. Serial sections of the minimally invasive adenocarcinoma from case 10 (listed in Fig. 2A and Supplementary Table S1) were stained with H&E (A) and immunostained with either the Notch2 or Six1 antibody (B). Representative staining images of the lepidic growth (LG) and microinvasion (MI) components are shown in the left and right panels, respectively. Bar, 100 μm.

morphology, NCI-H441 cells expressed easily and faintly detectable levels of *E-cadherin* and *vimentin*, respectively (Fig. 4A, lane 1). The expression levels of these two genes were inverse in NCI-H441 cells transfected with Notch2 ICD cDNA (Fig. 4A, lane 3 and Supplementary Fig. S2). Such transfection also resulted in *Smad3* and *Smad4* trans-activation (Fig. 4A, lane 3 and Supplementary Fig. S2). Transfection with the empty vector did not alter the endog-enous expression of these 4 genes (Fig. 4A, lane 2 and Supplementary Fig. S2). Transfection with TTF-1 resulted in *vimentin* transactivation and *E-cadherin* downregulation (Fig. 4A, lane 4 and Supplementary Fig. S2). Notch2 seemed to promote EMT in NCI-H441 cells more efficiently than TTF-1. NCI-H441 cells were transfected with Notch2 ICD cDNA and with either Six1-targeting siRNA or a control scrambled siRNA. The Six1-targeting siRNA abrogated not only Notch2 ICD–induced transactivation of *Six1* but also
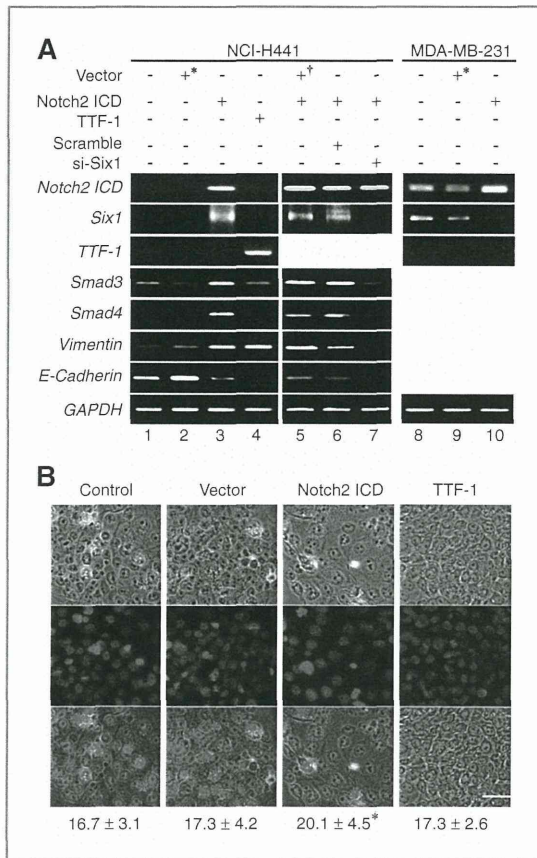
Clinical Cancer Research

Figure 4. Transcriptional and cell morphologic alterations induced by exogenous Notch2 ICD in NCI-H441 cells. A, expression of EMT-related genes in NCI-H441 and MDA-MB-231 cells before and after transfection with various transcription factors and si-RNA. NCI-H441 and MDA-MB-231 cells were transiently transfected with pCX4-bsr empty (*lanes 2 and 9) or with vectors expressing either Notch2 ICD (lanes 3 and 10) or TTF-1 (lane 4). NCI-H441 cells were transiently transfected in some experiments with Notch2 ICD cDNA and with either empty pSilencer4.1-CMVneo (†lane 5) or vectors expressing scrambled (lane 6) or Six1-targeting (lane 7) siRNA. Total RNAs extracted from intact or transfected cells were analyzed by RT-PCR using primer set for indicated genes. Portions of PCR products were resolved by electrophoresis on 1% agarose gels. B, changes in sizes of nuclei in NCI-H441 cells transfected with Notch2 ICD cDNA. NCI-H441 cells were transfected or not (control) with either empty pCX4-bsr or vectors expressing cDNAs for Notch2 ICD or TTF-1 and then stained with DAPI to visualize nuclei (blue). Phase-contrast (top) and UV laser (middle) images of cells are merged (bottom). Sizes of nuclei were determined as described in Materials and Methods, and calculated means and SE are shown below the images. *, P < 0.01 compared with values of other types of cells. Bar, 50 μm.

that of *Smad3*, *Smad4*, and *vimentin*, whereas it further enhanced the Notch2 ICD–induced downregulation of *E-cadherin* (Fig. 4A, lane 7). Control transfection did not alter the gene expression induced by Notch2 ICD (Fig. 4A, lanes 5 and 6). These results indicated that Six1 is essential for

Notch2 to transactivate *Smad3*, *Smad4*, and *vimentin*, but not to downregulate *E-cadherin*.

Notch2 ICD transfection experiments, followed by RT-PCR, were conducted on 2 other lung adenocarcinoma cell lines, A549 and RERF-LC-MS, both of which expressed endogenously undetectable levels of Notch2 and Six1 (Supplementary Fig. S3). Exogenous Notch2 ICD in these cells induced gene expression alterations resembling those in NCI-H441 cells, except that *Smad4* and *E-cadherin* were not upregulated in A549 and RERF-LC-MS, respectively (Supplementary Fig. S3). These results suggested that Notch2 and Six1 played pivotal roles in inducing EMT of lung adenocarcinoma cells.

Early-stage lung adenocarcinoma progression is assumed to be associated with an increase in the size of cancer cell nuclei (8). We measured the greatest dimension of cancer cell nuclei in 5 minimally invasive adenocarcinomas and found significantly larger nuclei in micro-invasion, than in lepidic growth cancer cells from all 5 minimally invasive adenocarcinomas (Supplementary Table S1). A comparison between intact NCI-H441 cells and those transfected with the Notch2 ICD cDNA showed significantly larger nuclei in the transfectants than in the intact cells (Fig. 4B). Transfection with empty vector or with TTF-1 cDNA did not alter the size of nuclei in NCI-H441 cells (Fig. 4B).

Upregulation of Notch2 and Six1 defines a clinically aggressive phenotype of lepidic-predominant invasive adenocarcinoma

We immunohistochemically analyzed 64 samples of lepidic-predominant invasive adenocarcinoma tumors using antibodies against Notch2 and Six1. Table 1 summarizes the clinicopathologic features of each case. The immunohistochemical staining results were judged positive when more than 50% of the cancer cells in each of the lepidic growth and overt invasion components had significant cytoplasmic (Notch2) or nuclear (Six1) staining. The tumors were classified based this judgment as double (Notch2 and Six1) negative in lepidic growth, but double positive in overt invasion (N/P; n = 23) cells; double negative in both components (N/N; n = 19); double positive in both components (P/P; n = 19) and other (n = 3; summarized in Table 1). A representative staining profile of N/P tumors was shown in Supplementary Fig. S4. A statistical analysis of the clinicopathologic parameters among the groups showed that the N/P group was less favorable than the N/N group with respect to pT, pN, PL factor, and ly factor (Table 1). Univariate log-rank analyses of Kaplan–Meier survival curves revealed that DFS duration was shorter in the N/P, than in the N/N group (P = 0.015; Fig. 5). DFS duration was also affected by various clinicopathologic parameters including pStage, pT, pN, PL factor, and ly factor (Supplementary Table S3). Multivariate logistic regression analyses among the 3 groups revealed that the N/P and P/P groups were more likely to recur than the N/N group in 2-year postoperative follow-up (Supplementary Table S4).

Table 1. Classification of patients with lepidic-predominant invasive adenocarcinoma according to Notch2 and Six1 immunohistochemical findings

Variable	All patients	Notch2 and Six1						P
		N/N	N/P	P/P	Other			
Sex						N/N vs. N/P	0.59
Male	36	10	14	11	1	N/N vs. P/P	0.74
Female	28	9	9	8	2	N/P vs. P/P	0.85
Age						N/N vs. N/P	0.95
Mean	71	70.5	70.7	70.8	78.3	N/N vs. N/P	0.93
Range	49–86	49–86	58–83	56–85	74–85	N/P vs. P/P	0.97
pStage[a]						N/N vs. N/P	0.33
IA + IB	52	17	18	14	3	N/N vs. P/P	0.21
IIA + IIB + IIIA + IIIB	12	2	5	5	0	N/P vs. P/P	0.73
pT[a]						N/N vs. N/P	0.04
1a + 1b	39	15	11	11	2	N/N vs. P/P	0.16
2a + 2b + 3	25	4	12	8	1	N/P vs. P/P	0.52
pN[a]						N/N vs. N/P	0.03
0	55	19	18	15	3	N/N vs. P/P	0.03
1 + 2	9	0	5	4	0	N/P vs. P/P	0.96
PL factor[a]						N/N vs. N/P	0.005
0	50	18	13	17	2	N/N vs. P/P	0.55
≥1	14	1	10	2	1	N/P vs. P/P	0.02
ly Factor[a]						N/N vs. N/P	0.039
0	46	18	16	10	2	N/N vs. P/P	0.003
1	18	1	7	9	1	N/P vs. P/P	0.26
v Factor[a]						N/N vs. N/P	0.67
0	56	18	21	14	3	N/N vs. P/P	0.08
1	8	1	2	5	0	N/P vs. P/P	0.13
Tumor size (mm)						N/N vs. N/P	0.89
Mean	25.3	25.5	25	24.7	30	N/N vs. P/P	0.82
Range	11–70	11–70	15–40	12–38	15–50	N/P vs. P/P	0.87

[a]According to TNM classification (7th Edition).

Discussion

This study comprised 3 parts. A clinical issue had to be considered for the first part that compared comprehensive gene expression between lepidic growth and microinvasion cancer cells in individual minimally invasive adenocarcinomas. Because the cut surface at the greatest dimension of the tumor is used for pathologic diagnosis, remaining specimens for LMD contained only a small amount of each component, particularly the microinvasion component. The original estimated amount of total RNA used for the present DNA microarray analysis was in the order of 100 ng per component or less. This limitation might have caused considerable RNA degradation and consequently resulting in shorter aRNA probes (theoretical average length, ~1.5 kb) (Fig. 1C). Regardless, the DNA microarray analysis seemed reliable because (i) the range of the relative expression levels of 10 housekeeping genes was sufficiently small
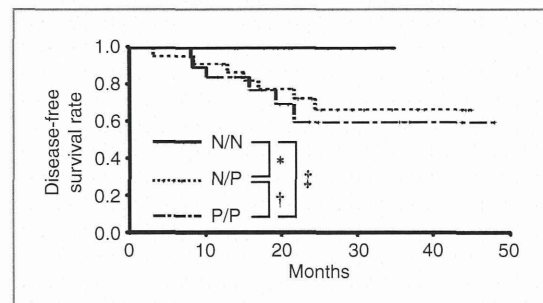

Figure 5. DFS rates of 64 lepidic-predominant invasive adenocarcinomas grouped by Notch2 and Six1 immunohistochemistry. DFS rates of N/N, N/P, and P/P tumor groups shown as function of months. The mean interval of DFS (95% CI) for N/P and P/P are 34.9 (28.8–41.1) months and 34.7 (26.2–43.2) months, respectively. Values for N/N were not calculated because N/N tumors did not recur. *, $P = 0.015$; †, $P = 0.626$; ‡, $P = 0.006$.

(within 0.5- to 2-fold) between lepidic growth and micro-invasion cells (Supplementary Table S2), and (ii) differential expression of the selected 2 genes, that is, *Notch2* and *Six1* genes, was reproducibly confirmed by RT-PCR (Fig. 2A, case 1). These results indicate that tumor lesions at the early stage that contain cancer cells with different malignant potential, for example, *in situ* and invasive cells in minimally invasive adenocarcinoma, are practical for comparative gene expression analyses among cancer cells during progression *in vivo*.

Both *Notch2* and *Six1* were upregulated in microinvasion cancer cells not only in the minimally invasive adenocarcinoma that was analyzed using DNA microarrays but also in 10 other minimally invasive adenocarcinomas examined. We therefore considered that paired upregulation of Notch2 and Six1 is commonly associated with the progression of lepidic growth to microinvasion cancer cells in minimally invasive adenocarcinoma. Notch2 is a cell membrane–bound ligand-dependent receptor for the Type 1 transmembrane protein family named Notch (30–33). When Notch ligands bind to Notch2 receptors between two neighboring cells, Notch2 is cleaved through a cascade of proteolytic enzymes, including γ-secretase, and released Notch2 ICD translocates into the nucleus where it transcriptionally activates Notch2 target genes (26). Although Notch1 and Notch3, other members of the Notch family, have long been regarded as candidate molecules responsible for the development of lung cancer (34–36), whether Notch2 has similar roles remains to be determined. Six1 is a homeodomain transcription factor (37) and a putative downstream target of Notch2 (24, 25). Interestingly, Ford and colleagues showed that Six1 stimulates the malignant transformation of mammary epithelial cells through trans-activating *cyclin A1* (38, 39) and induces EMT in mammary cancer cells through the induction of TGF-β signaling (27, 40). These findings suggested that Notch2 and Six1 play coordinate roles during the early-stage lung adenocarcinoma progression.

The second part of this study examined this notion using transfection experiments. Consistent with previous characterization, exogenous expression of the Notch2 ICD resulted in *Six1* transactivation in NCI-H441 lung epithelial cells. The exogenous Notch2 ICD also transactivated *Smad3*, *Smad4*, and *vimentin* in association with the downregulation of *E-cadherin*. Similar transactivation effects of Notch2 ICD were detected in 2 other types of epithelial cells derived from lung adenocarcinomas. Interestingly, Six1 was notably essential for transactivation of the 3 genes, but not for the downregulation of *E-cadherin*, suggesting that Notch2 and Six1 coordinately played a causative role in inducing EMT during the progression of lepidic growth to microinvasion cells. Exogenous expression of the Notch2 ICD in NCI-H441 cells also resulted in nuclei becoming enlarged. This was in accordance with the cytologic finding that nuclei were larger in microinvasion cancer cells than in lepidic growth cells from 5 minimally invasive adenocarcinomas examined. These results supported the notion that the transcriptional cascades activated coordinately by Notch2

and Six1 are involved in lepidic growth-to-microinvasion progression.

The third part of the study immunohistochemically investigated Notch2 and Six1 in 64 samples of lepidic-predominant invasive adenocarcinoma tumors and found that they could be assigned almost equally into groups on the basis of positive and negative staining as N/N, N/P, and P/P. Consistent with the results of the second part of the study showing that Six1 is a downstream target of Notch2, these transcription factors were either double negative or double positive in lepidic growth and overt invasion cancer cells, respectively, with some exceptions. As might be predicted from the diagnostic criteria, lepidic-predominant invasive adenocarcinoma seemed to include heterogeneous tumors with distinct natural histories and genetic alterations. Judging from the immunostaining profiles of lepidic growth and overt invasion cells, N/P tumors seem to be a simple advanced form of minimally invasive adenocarcinoma, in which microinvasion cells have grown into an overt invasion focus, and N/N tumors develop via other molecular mechanisms than those involving Notch2 and Six1. On the other hand, the origin of P/P tumors is uncertain, but they might be a more advanced form of N/P tumors. Because lepidic growth cancer cells were positive for both Notch2 and Six1, they might be potentially invasive. This speculation is reminiscent of a recent report by Anami and colleagues who notably pointed out that the lepidic growth pattern might represent the intraalveolar epithelial spread of overt invasion cancer cells (41). Whether or not lepidic growth cancer cells are invasive did not seem to affect the prognostic outcomes of patients with lepidic-predominant invasive adenocarcinomas (N/P vs. P/P in Fig. 5). Interestingly, we found that N/N tumors metastasized less often to lymph nodes, were less invasive to lymphatic vessels, and were associated with better DFS than N/P and P/P tumors ($P = 0.015$ and 0.006 by log-rank tests, respectively). These findings agree with a summary of reviews that emphasize the critical role of Notch signals in the malignant progression of non-small cell lung cancer (34–36). The paired upregulation of Notch2 and Six1 seemed to be one transcriptional alteration that is responsible for minimally invasive adenocarcinoma-to-lepidic-predominant invasive adenocarcinoma progression, and it defined a clinically aggressive phenotype subset of lepidic-predominant invasive adenocarcinoma. Because Notch2 and Six1 immunohistochemistry seemed to independently discriminate lepidic-predominant invasive adenocarcinomas with high risk of recurrence in a 2-year postoperative period, during which the recurrence of most lung cancers occurs even after curative-intent therapy (42), it could be a clinically useful examination for selecting patients with lepidic-predominant invasive adenocarcinoma needing intensive follow-up.

Aviel-Ronen and colleagues (2008) examined genomic changes associated with adenocarcinoma *in situ* and minimally invasive adenocarcinoma using array comparative